

Response modification factors of concrete bridges with different bearing conditions

Seyed Mehdi Zahrai^{*1}, Amir Khorraminejad^{2a} and Parshan Sedaghati^{3b}

¹School of Civil Engineering, College of Engineering, The University of Tehran, Tehran, Iran

²Department of Civil Engineering, Shahid Beheshti University, Tehran, Iran

³Department of Civil Engineering, Semnan University, Semnan, Iran

(Received September 22, 2017, Revised December 30, 2018, Accepted January 13, 2019)

Abstract. One of the shortcomings of seismic bridge design codes is the lack of clarity in defining the role of different seismic isolation systems with linear or nonlinear behavior in terms of R -factor. For example, based on AASHTO guide specifications for seismic isolation design, R -factor for all substructure elements of isolated bridges should be half of those expressed in the AASHTO standard specifications for highway bridges (i.e., $R=3$ for single columns and $R=5$ for multiple column bent) but not less than 1.50. However, no distinction is made between two commonly used types of seismic isolation devices, i.e., elastomeric rubber bearing (ERB) with linear behavior, and lead rubber bearing (LRB) with nonlinear behavior. In this paper, five existing bridges located in Iran with two types of deck-pier connection including ERB and LRB isolators, and two bridge models with monolithic deck-pier connection are developed and their R -factor values are assessed based on the Uang's method. The average R -factors for the bridges with ERB isolators are calculated as 3.89 and 4.91 in the longitudinal and transverse directions, respectively, which are not in consonance with the AASHTO guide specifications for seismic isolation design (i.e., $R=3/2=1.5$ for the longitudinal direction and $R=5/2=2.5$ for the transverse direction). This is a clear indicator that the code-prescribed R -factors are conservative for typical bridges with ERB isolators. Also for the bridges with LRB isolators, the average computed R -factors equal 1.652 and 2.232 in the longitudinal and transverse directions, respectively, which are in a good agreement with the code-specified R -factor values. Moreover, in the bridges with monolithic deck-pier connection, the average R -factor in the longitudinal direction is obtained as 2.92 which is close to the specified R -factor in the bridge design codes (i.e., 3), and in the transverse direction is obtained as 2.41 which is about half of the corresponding R -factor value in the specifications (i.e., 5).

Keywords: response modification factor; concrete bridge; nonlinear static analysis; nonlinear time-history analysis; seismic isolator; ductility; seismic design

1. Introduction

Performance of bridge structures as the vital transportation arteries, particularly in emergency situations such as seismic events, has always been an important issue. Recent earthquakes in different countries, specifically the Northridge and Imperial Valley (U.S.) and the Kobe (Japan), have shown that the designed bridges according to the existing codes have experienced extensive damage, while recorded ground motions demonstrated that the intensities of those earthquakes were less than the corresponding values in the design codes. This deficiency in the bridge's performance is due to the elastic design concept that the codes reduce the actual seismic forces and use specific operational details to enhance the ductility of lateral load resisting elements in order to consider the actual nonlinear behavior of bridges during earthquakes. Seismic

isolation is a passive control system which reduces seismic forces acting on the substructure.

Elastomeric Rubber Bearing (ERB) and Lead Rubber Bearing (LRB) are two common types of isolation systems that have different natures for seismic mitigation. Using LRB isolators result in a significant reduction in the transmission of forces between the bridge superstructure and substructure (Kelly 1997, Naeim and Kelly 1999). This reduction of forces allows the bridge to remain in the elastic range and eliminates the occurrence of plastic hinges in bridge columns. ERB is the only single-unit isolation system, among common isolators, which has both linear restoring force and linear damping (Skinner *et al.* 1993). Both ERB and LRB isolators protect the bridge from earthquake ground motions by increasing the structure fundamental period (or modal damping). But LRB dissipates seismic energy through additional hysteretic damping by yielding of the lead plug. The nonlinear behavior of LRB isolators is significant due to yielding of the substructure elements causing a direct effect on ductility and energy dissipation.

Many researchers have assessed different types of bearings incorporated in isolated bridges. Saïidi *et al.* (1999) investigated the hysteretic behavior of isolated bridges with elastomeric isolators with or without lead

*Corresponding author, Professor

E-mail: mzahrai@ut.ac.ir

^aPh.D. Student

E-mail: a_khorraminejad@sbu.ac.ir

^bPh.D. Student

E-mail: psedaghati@semnan.ac.ir

cores. They showed that properly designed isolators can reduce the ductility demand in RC bridge columns. Olmos (2008) confirmed the beneficial effects of lead rubber isolators through an analytical study on the seismic response of 36 bridges considering models with and without base isolators, structures with linear base isolators and bridges with nonlinear isolators. In a similar study, Olmos *et al.* (2011) assessed the effectiveness of the nonlinear lead-rubber bearings on reducing the seismic demands of eight generic base isolated bridge models designed for hard and medium soil types. Losanno *et al.* (2014) suggested a theoretical approach for determining the optimal value of the inherent viscous damping in case of viscoelastic isolators, or the yielding force in case of sliding isolators. Toopchi-Nezhad (2014) presented simplified analytical models for the unbonded fiber reinforced elastomeric bearing (U-FREB). Amiri *et al.* (2016) proposed a direct displacement-based design method for a continuous deck bridge isolated with triple friction pendulum bearings (TFPB). They concluded that the proposed procedure is able to predict seismic demands with acceptable accuracy. Kataria and Jangid (2016) investigated the effectiveness of hybrid systems by applying a smart semi-active piezoelectric friction damper (PFD) for seismic control of horizontally curved bridges isolated with LRB. They deduced that the use of semi-active PFD with LRB is quite effective in controlling the response of the curved bridge as compared with passive systems. Roy *et al.* (2016) discussed the optimum design of seismic isolation system of a simply supported isolated bridge through a statistical linearization framework by considering the effect of excessive isolator displacement. Al-Anany *et al.* (2017) investigated the seismic response of a typical highway bridge isolated using the unbonded fiber reinforced elastomeric isolator (U-FREI) and compared it to a non-isolated bridge with a monolithic connection between the superstructure and substructure. They indicated that U-FREI has the potential to efficiently improve the seismic response in highway bridges during a seismic event; since all the bridge components, particularly the columns, remained within its elastic range with no yielding or plastic hinge damage in the isolated bridge.

According to the bridge design practices such as AASHTO standard specifications for highway bridges, the design displacement demand of connections between the superstructure and substructure (ERBs and LRBs) are obtained based on the non-reduced seismic forces in order to prevent bearing failure and superstructure unseating. Besides, the nonlinear demand such as ductility and energy dissipation in linear analysis is considered by the response modification factor (R) in US codes and behavior factor (q) in Eurocode 8.

As specified in Eurocode 8, values for q of concrete bridges depend on whether the bridge is designed as “ductile” or “limited ductile”. For ductile concrete bridges with vertical piers $q=3.5\lambda(\alpha_s)$ that has a maximum value of 3.5 ($\alpha=L_s/h$ is the shear span ratio of the pier, where L_s is the distance from the plastic hinge to the point of zero moment and h is the depth of the cross section in the direction of flexure of the plastic hinge). For bridges with seismic isolation, q -factor value shall be assumed as “limited

ductile” ($q\leq 1.5$). Also in AASHTO guide specifications for seismic isolation design, R -factor for all parts of substructure should be equal to half of the R -factor values in conventional design (without isolation), but R -factor should not be less than 1.5. For instance, R -factor equals 3.0 for single column pier, and in the case of using seismic isolators, $R=1.5$. On the other hand, in some specifications such as Specification No.463 (Standard Loads for Bridges, 2000), the effect of using elastomeric rubber bearing (ERB) or lead rubber bearing (LRB), on the R -factor value is not mentioned. Itani *et al.* (1997) investigated the effect of three parameters on the response modification factors for single column circular reinforced concrete bridge bents. They concluded that increase in the longitudinal reinforcement ratio results in a reduction of R value. Also it was found that the R -factors determined for different capacity to demand displacement ratios were very sensitive to the period and did not show a consistent trend. Besides, they showed that doubling the minimum confining steel had only a slight effect on the response modification factor.

Constantinou and Quarshie (1998) discussed the rationale for the lower R -factors that have been specified for seismically isolated bridges in AASHTO. Dynamic analyses were conducted on a number of simple two-degree-of-freedom models of both seismically isolated and non-isolated bridges. The authors concluded that the R -factors of substructures of isolated bridges should be in the range of 1.5 to 2.5 which are similar to the recommended values presented in the AASHTO Guide Specifications for seismic isolation design. Memari *et al.* (2005) studied the displacement ductility and force reduction factor for five existing bridge models with single and multiple column bents through pushover analyses. For the bridges studied, R -factor values ranging from 1.75 to larger than 3 were obtained.

Kappos *et al.* (2013) conducted a research to evaluate the response modification factors (q -factor) of bridges in Europe considering the seismic energy dissipation mechanism. They considered bridges in two categories including bridges with yielding piers and bridges with elastomeric bearing connection between superstructure and substructure (non-yielding piers). For bridges of the first category, q -factor was estimated as the product of ductility and overstrength factors. For bridges of the second category, q was defined as the ratio of the spectral acceleration (corresponding to the pertinent predominant period of the bridge) for which failure occurs to the design spectral acceleration. The estimated q -factors for concrete bridges with yielding piers varied from 4.2 to 10.1 in the longitudinal direction and from 3.7 to 11.6 in the transverse direction. Also, for the bridges on elastomeric bearings the q values were in the range of 4 to 6.6 and 4.3 to 9.3 in the longitudinal and transverse directions, respectively. The authors expressed that code-specified values are not only feasible but in several cases are actually an underestimation of the actual energy dissipation capacity of the bridge. Also these higher q values than those used for design is a clear indication that modern bridges possess adequate margins of safety.

Soares *et al.* (2017) studied the effect of axial force,

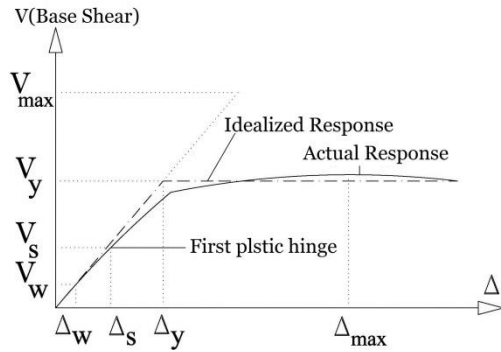


Fig. 1 Schematic force-displacement behavior of a conventional structure (Uang 1991)

volumetric transverse reinforcement and soil-structure interaction on reinforced concrete bridge pier ductility (μ). They concluded that ductility capacity increases as the transverse reinforcement increases. Also, the increase in axial compression force, the pier ductility decreases. In addition, the precise modeling of deep foundations, including piles, pile cap, and springs to simulate the soil-structure interaction results in greater ductility values compared to that of fixed piles.

In the previous research works, R -factor value, ductility and overstrength factors are studied for the isolated and non-isolated bridges. But differences between two commonly used types of base isolation devices, i.e., ERB and LRB have not been discussed yet. Different seismic responses result from linear and nonlinear isolation systems. In fact, the linear behavior of ERB causes formation of plastic hinges in piers, but nonlinear behavior of LRB leads to linear performance in the substructure.

This paper attempts to evaluate R -factor values of isolated bridges in two cases of using ERB isolator (linear behavior) and LRB isolator (nonlinear behavior) as the bridge bearings in order to compare the results with those prescribed by the bridge design codes. According to AASHTO guide specifications for seismic isolation design, R -factor for all substructure elements of isolated bridges should be half of those expressed in the AASHTO standard specifications for highway bridges; however differences between the linear and nonlinear behavior of isolators are not considered.

To this end, five simple span existing bridge models with ERB and LRB isolators are developed. Also, in order to investigate the effect of deck to pier connection type on the R -factor value, two bridge models with voided slab deck monolithically attached to the piers are developed. LRB isolators are designed by using nonlinear time history analyses and also the seismic behavior of bridge models is compared. For computing R -factor values, static nonlinear push-over analysis is performed based on the Uang's theory.

2. Response modification factor

The main purpose of seismic design of structures is based on two basic criteria. First, under low earthquakes, the structural behavior must remain in the elastic range

without damages. Second, under severe earthquakes, while retaining the overall stability of structure, structure should tolerate the earthquake-induced damages. Seismic resistance of structures designed based on the seismic design codes, is generally much less than the lateral resistance which is required to provide the structural stability in elastic range during a severe earthquake. So during strong earthquakes, structures experience nonlinear behavior and therefore nonlinear analysis is required for design purposes. However, due to the simplicity of elastic method, conventional methods of analysis are based on linear analysis considering the reduced seismic forces. Schematic force-displacement behavior of a conventional structure is depicted in Fig. 1. This reduced seismic force is obtained by dividing the elastic base shear by R -factor. In other words, in linear analysis, the elastic base shear force level (V_e), is reduced to the force level corresponding to the formation of the first plastic hinge in the structure (V_s).

2.1 The Uang's ductility coefficient method

One of the most reliable methods for computing R -factor is presented by Uang (1991). The maximum base shear is calculated when the structure remains in the elastic range. The response modification factor consists of two parts: a reduction factor due to ductility (R_μ) and an overstrength coefficient (Ω). R_μ is the ratio of base shear at elastic level (V_e) to the base shear at the level of structural failure (V_y); and Ω is defined as the ratio of the base shear at strength level which corresponds to the formation of a yield mechanism (V_y) to the base shear of structure when the first plastic hinge is formed (V_s). According to Fig. 1 the required elastic resistance due to the base shear coefficient is determined by Eq. (1).

$$C_e = \frac{V_e}{W} \quad (1)$$

Where W is the effective structural weight, and V_e is the maximum base shear when the structure is in the elastic range. Regarding the Uang's method, the required equations for calculating R -factor are as follows

$$\Omega = \frac{V_y}{V_s} \quad (2)$$

$$R_\mu = \frac{V_e}{V_y} \quad (3)$$

$$R = \frac{V_e}{V_s} = \frac{V_e}{V_y} \times \frac{V_y}{V_s} = R_\mu \Omega \quad (4)$$

3. Analytical modeling

Five simple span existing bridge models with ERB isolators between substructure and superstructure are developed for assessing the R -factor values. Also in another case, the ERBs were replaced by LRB isolators and their R -factor values are obtained. Furthermore, two existing

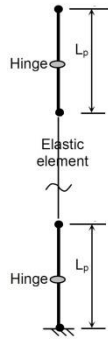


Fig. 2 Assignment of plastic hinges to plastic hinge zones (Aviram *et al.* 2008)

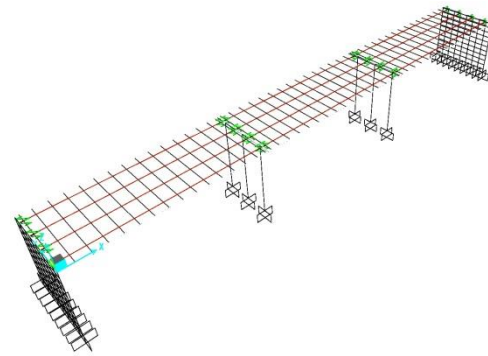


Fig. 3 Three-dimensional finite element model of bridge model 1 in CSiBridge 2015

bridges with voided slab deck monolithically connected to the piers are developed and values for *R*-factors are evaluated. When conducting nonlinear analysis, it is necessary to consider nonlinear behavior of all elements that are prone to behave nonlinearly. This is mainly achieved by assigning plastic hinges to bridge columns. For all analytical bridge models, plastic hinges are modeled at top and bottom of piers. The plastic hinge length (*L_p*) is determined according to Eq. (5) (Caltrans 2010)

$$L_p = 0.08L + 0.022f_{ye}d_{bl} \geq 0.044f_{ye}d_{bl} \quad (5)$$

Where *L* is the column length; *f_{ye}* denotes the expected yield strength of longitudinal reinforcement; and *d_{bl}* represents the nominal bar diameter of longitudinal reinforcement. Plastic hinges are assigned at the mid-height of plastic zone with a segmental length *L=L_p* as shown in Fig. 2 (Aviram *et al.* 2008).

The bridges were developed with a three-dimensional model in CSiBridge 2015 software (Computers and Structures, Inc. CSI 2015). Properties of the bridge models are listed in Table 1. For modeling the girders and piers, the “Frame” element is used. The concrete slab of the bridge models 1 to 5 is modeled with the “Frame” element and the slab of the bridge models 6 and 7 is modeled with the “Shell” element. ERB is modeled with linear spring, and LRB is modeled with nonlinear Link (Rubber isolator). An example of the finite element modeling of the bridge model 1 is depicted in Fig. 3.

LRB isolator’s behavior is considered as a bilinear hysteretic idealized model which has nonlinear properties at the shear degree of freedom, and linear properties at the other degrees of freedom. Nonlinear models are considered according to the hysteretic behavior proposed by Wen (1976), Park *et al.* (1986), and the model used for analyzing the isolated structures are considered with regards to the proposed approach of Nagarajaiah *et al.* (1991). According to this method, the required parameters for LRB modeling are as follows:

- Effective stiffness in the elastic range (*K_{eff}*) at degrees of freedom with linear properties.
- Initial stiffness in the inelastic range (*K_u*) which is considered at degrees of freedom with nonlinear properties.
- Yielding strength (*F_y*) and the ratio of isolator stiffness after yielding to the initial stiffness (*K_d/K_u*). These two parameters are applied to the degrees of freedom with nonlinear characteristics.

Dead loads and live loads for the seven bridge models in Table 2 are considered based on the Specification No. 463 (Road and Railway Bridges Seismic Resistant Design Code, 2008), and Specification No. 139 (Standard Loads for Bridges, 2000). Specification No. 139 is used for the gravity loads and Specification No. 463 is used for the seismic loads. Dead loads consist of two components: Primarily, dead loads include the weight of the girders, concrete slab, diaphragms and connections. Secondly, dead loads include loads of the barriers, sidewalks, asphalt and curbs. These

Table 1 General properties of the Bridge models

Bridge ID	Bridge 1	Bridge 2	Bridge 3	Bridge 4	Bridge 5	Bridge 6	Bridge 7
Bridge name	30-milely	Bakhtiari river	Zal	Aab-lashgar	Ajorlou	Binaloud-1	Binaloud-2
No. of spans	3	3	5	3	6	2	2
Span length(m)	3×30	2×15+50	5×20	3×22	6×22	2×16.5	2×16.5
Bridge width	11.80	8.80	13.60	11.80	11.80	14.90	28.20
No. of girders	4	4	6	6	6	Voided slab Deck	Voided slab Deck
Girder material	Steel	Steel	Concrete	Concrete	Concrete	Concrete	Concrete
No. of piers	3	2	3	2	2	2	4
Pier Height(m)	11.70	12.40	6.20 & 10.70	12.35 & 12.65	7.16	8.5	8.5
Pier diameter (m)	<i>D</i> =1.50	<i>D</i> =1.50	<i>D</i> =1.50	<i>D</i> =1.50	<i>D</i> =1.50	1.25×2.0	1.25×2.0

Table 2 Dead loads and Live loads of bridge models

Bridge case model	1	2	3	4	5	6	7
Dead Load (kN)	13180	6470	14960	10640	19300	9220	54360
Live Load (kN)	3020	2720	4980	2380	3890	2700	6020

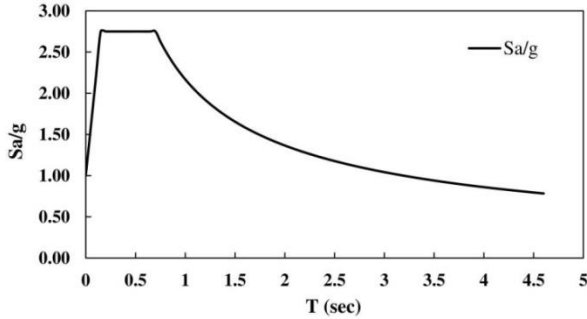


Fig. 4 Elastic design spectrum according to Specification No. 463 for Soil type III

loads are calculated for each bridge separately. According to the Specification No.139, there are four kinds of live loads, including a forty-ton truck, a ninety-ton tractor trailer, a seventy-ton tank, and a uniform load of 1.50 ton/m. Dynamic spectral analysis according to the Specification No. 463 is used in order to calculate the seismic loads of the bridge models. The design response spectrum for soil type III is shown in Fig. 4, where the horizontal and vertical axes represent natural period and (S_d/g), respectively.

4. ERB modeling parameters

In order to model the ERB isolators, linear element is considered. Shear stiffness (K_s), vertical stiffness (K_v), and shape coefficient (S) of the linear element are computed from the following equations

$$K_s = \frac{GA}{T_r} \quad (6)$$

$$K_v = \frac{EA}{nt_i} \quad (7)$$

$$S = \frac{BL}{2t_i(B+L)} \quad (8)$$

where G is the shear modulus, A is the ERB's area, T_r is the total thickness of the rubber layers, E is the effective modulus of ERB in compression, t_i is the thickness of individual layer, L and B are the length and width of the isolator, n is the number of elastomeric layers and H is the total height of the isolator respectively. Analytical parameters and geometrical properties of ERB for the bridge models are presented in Table 3.

5. LRB isolator design

For analysis and design of LRB isolators, it is necessary

Table 3 ERB modeling parameters

	L (cm)	B (cm)	H (cm)	t_i (mm)	T_r (cm)	t_s (mm)	n	S	G (kN/m ²)	K_s (kN/m)	K_v (kN/m)
Bridge 1	40	20	5.2	8	3.7	3	4	8.33	1000	2119	1052123
Bridge 2a	40	30	8.5	8	6.1	3	7	10.7	1000	1933	1599069
Bridge 2b	25	20	3.0	8	2.1	3	2	6.94	1000	2335	985385
Bridge 3	30	20	5.2	8	3.7	3	4	7.5	1000	1589	675752
Bridge 4	40	20	4.1	8	2.9	3	3	8.33	1000	2708	1402830
Bridge 5	40	20	4.1	8	2.9	3	3	8.33	1000	2708	1402830
Bridge 6	40	25	6.3	8	4.5	3	5	9.62	1000	2178	1466193
Bridge 7	40	25	6.3	8	4.5	3	5	9.62	1000	2178	1466193

a: Shorter Span ; b: Longer Span

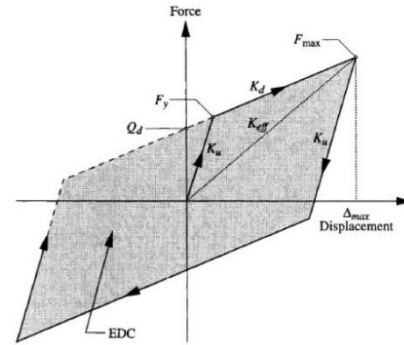


Fig. 5 Bilinear hysteretic idealized model for the LRB isolator (Naeim and Kelly 1999)

to know the parameters such as shear force, maximum displacement, elastic stiffness (initial stiffness), stiffness after yielding (secondary stiffness), and yielding force of isolators. As shown in Fig. 5, behavior of the LRB isolators can be considered as a bilinear model.

K_u is the elastic (unloading) stiffness; K_d is the post-elastic stiffness (secondary stiffness); K_{eff} is the isolator's effective stiffness; F_y is the yield force; F_{max} is the maximum force; Δ_{max} is the maximum isolator displacement; Q_d is the characteristic displacement; and EDC represents energy dissipation per cycle or area of hysteresis loop (shaded).

The design procedure of the LRB seismic isolators according to AASHTO guide specifications for seismic isolation design is represented in Fig. 6 and is summarized as follows:

- i. Initial values for elastic stiffness (K_u), secondary stiffness (K_d), yielding force (F_y), and maximum LRB isolator's displacement (d) must be assumed. First assumption of " d " is based on the results of the nonlinear time history analysis of the isolated bridges.

In order to determine the maximum displacement of LRB isolators (d), nonlinear time-history analyses are conducted with seismic inputs including seven pairs of ground motions including the Tabas, Manjil, Imperial Valley, Northridge, Kobe, Loma Prieta and San Fernando earthquakes. Characteristics of the selected earthquake records are presented in Table 4. Based on the seismic design practices such as Specification No.463, if nonlinear time-history analysis is selected as the analysis method, at least three pairs of scaled horizontal ground motion time-history components shall

Table 4 Characteristics of the selected ground motion records

Earthquake	Not Scaled PGA		Earthquake Magnitude (M_w)	Year	Fault type
	Longitudinal	Transverse			
Tabas	0.836 g	0.852 g	7.4	1978	Reverse
Manjil	0.515 g	0.462 g	7.4	1990	Strike slip
Imperial Valley	0.775 g	0.588 g	6.5	1979	Strike slip
Northridge	0.43 g	0.495 g	6.7	1994	Reverse
Kobe	0.238 g	0.212 g	6.9	1995	Strike slip
Loma Prieta	0.513 g	0.428 g	6.9	1989	Reverse Oblique
San fernando	0.21 g	0.182 g	6.6	1971	Reverse

be used. Maximum responses are then obtained for designing procedure. Also the code allows the consideration of the mean responses when non-linear dynamic analysis is performed for at least seven scaled independent ground motions. The scaling methodology is explained in subsection 5-1.

ii. Effective stiffness (K'_{eff}) of each LRB isolator is determined according to Eq. (9). Then the effective stiffness of the whole isolated structure (K_{eff}), that is the resultant stiffness of the isolators and substructure (K_{sub}), is calculated with regard to Eq. (10).

$$K'_{eff} = \frac{[F_y + K_d(d - \frac{F_y}{K_u})]}{d} \quad (9)$$

$$K_{eff} = \sum \left(\frac{K_{sub} \times K'_{eff}}{K_{sub} + K'_{eff}} \right) \quad (10)$$

iii. The effective period of the whole isolated structure (T_{eff}) is determined according to Eq. (11). Then the damping coefficient (B) can be calculated from Eq. (12). W is the bridge's weight, g is the acceleration due to the gravity, A is the spectral acceleration coefficient, and S_i is the site coefficient in the following equations.

$$T_{eff} = 2\pi \sqrt{\frac{W}{K_{eff} \times g}} \quad (11)$$

$$d = \frac{250 AS_i T_{eff}}{B} \quad (12)$$

iv. The equivalent viscous damping for the isolation system (β) is determined from Eq. (13), where "EDC" is the enclosed area of the hysteretic response of LRB isolator in Fig. 5, and d_i is the maximum displacement of the " i^{th} " isolator.

$$\beta = \frac{1}{2\pi} \times \frac{EDC}{\sum (K_{eff} \times d_i^2)} \quad (13)$$

v. Knowing the equivalent viscous damping, B coefficient can be determined from Table 5 according to the AASHTO guide specifications for seismic isolation design.

Table 5 Damping coefficient (B) (AASHTO 2014)

B	Damping (Percentage of Critical)						
	≤ 2	5	10	20	30	40	50
	0.8	1	1.2	1.5	1.7	1.9	2

vi. The obtained values of B coefficient from steps (3) and (5) are compared. If the change is notable, then a new value for the maximum isolator displacement (d) is considered and the above steps need to be repeated until the convergence is achieved.

vii. With regard to the value of (d), bridge's weight, and other parameters, the initial dimensions of LRB isolator such as length, width, thickness of a single rubber layer, number of layers, and the total thickness of layers are obtained in such a way that the following conditions are satisfied. γ_c , $\gamma_{s,s}$, $\gamma_{s,eq}$, γ_r are the various components of shear strains in the bearing that are calculated based on chapter 14 of the AASHTO guide specifications for seismic isolation design. γ_c is the shear strain due to vertical loads, $\gamma_{s,s}$ is the shear strain due to non-seismic lateral displacement, $\gamma_{s,eq}$ is the shear strain due to total design displacement (including shrinkage, creep, temperature and earthquake-induced displacement), and γ_r is the shear strain due to imposed rotation.

$$\gamma_c \leq 2.5 \quad (14)$$

$$\gamma_c + \gamma_{s,s} + \gamma_r \leq 5.0 \quad (15)$$

$$\gamma_c + \gamma_{s,eq} + 0.5\gamma_r \leq 5.5 \quad (16)$$

viii. Regarding the initial design of LRB isolators based on the nonlinear time history analysis, the maximum displacement of isolator (d_i), will be replaced by the initial assumed values of d . Then by repeating the above steps, the effective stiffness and the equivalent viscous damping ratio are obtained.

ix. Elastic stiffness of LRB isolators (K_u), must be greater than K_s in Eq. (17). K_s is the shear stiffness, G is the shear modulus, A is the isolator's area, and T_r is the total thickness of the rubber layers.

$$K_u \geq K_s = GA/T_r \quad (17)$$

x. Vertical stiffness of the isolator (K_v) can be calculated from Eq. (18); it is much greater than the horizontal stiffness. E_c is the effective modulus of elastomeric bearing in compression that is determined for rectangular isolators from Eq. (19). S is the shape factor of isolator which is better to be considered between 8 and 12 in order to gain the ratio of vertical stiffness to the horizontal stiffness about 400.

$$K_v = E_c A/T_r \quad (18)$$

$$E_c = 4GS^2 \quad (19)$$

With regard to the design procedure above, the design parameters of LRB isolators are determined based on their force and maximum displacement. Geometric properties, the modeling parameters of the designed LRB isolators, and

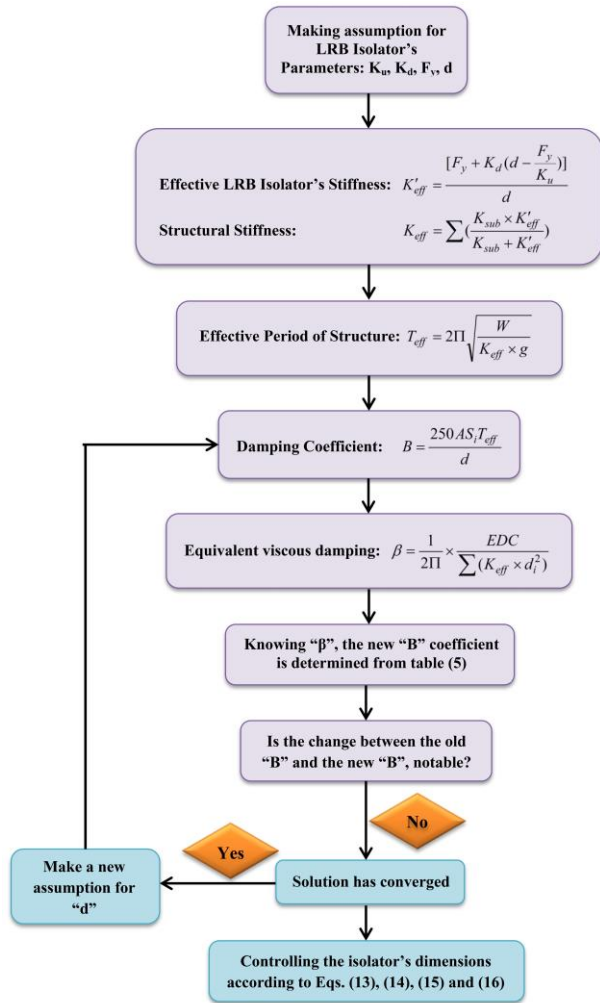


Fig. 6 Design procedure of LRB isolator based on AASHTO guide specifications for seismic isolation design

Table 6 Geometric properties of LRB isolators

	<i>L</i> (cm)	<i>B</i> (cm)	<i>h</i> (cm)	<i>t_i</i> (mm)	<i>T_r</i> (cm)	<i>t_s</i> (mm)	<i>n</i>	<i>S</i>	<i>G</i> (kN/m ²)
Bridge 1	35	35	13	10	11	2	11	8.75	1000
Bridge 2	35	35	16.6	12	14.4	2	12	7.29	1000
Bridge 3	30	30	7.8	8	6.4	2	8	9.375	1000
Bridge 4	35	30	17.8	10	15	2	15	8.08	700
Bridge 5	35	35	16.6	10	14	2	14	8.75	1000

the controlling AASHTO criteria are presented in Tables 6-8, respectively.

5.1 Accelerogram-scaling procedure

When a nonlinear time-history analysis is carried out, the scaling procedure of the chosen set of accelerograms should match the following criteria according to Code NO. 463:

- All of the accelerograms shall be scaled so that the pick ground acceleration (PGA) equals the gravitational acceleration (*g*).
- For each earthquake consisting of a pair of horizontal motions, the SRSS spectrum shall be established by

Table 7 Design parameters of LRB isolators

	<i>N</i>	<i>K_{eff}</i> (kN/m)	<i>T_{eff}</i> (sec)	<i>β%</i>	<i>K_u</i> (kN/m)	<i>F_y</i> (kN)	<i>K_d/K_u</i>
Bridge 1	24	33802	1.998	15	10648	122.4	0.1
Bridge 2	24	13553	2.24	5	5199	31.3	0.1
Bridge 3	60	120413	1.145	15	15173	61.3	0.1
Bridge 4	36	20090	2.5	12	4500	56.6	0.1
Bridge 5	72	71622	1.67	12	8023	53.2	0.1

Table 8 Controlling AASHTO criteria for LRB isolator design

	<i>γ_c</i>	<i>γ_r</i>	<i>γ_s</i>	<i>γ_{s,eq}</i>	Eq. (14)	Eq. (15)	Eq. (16)
Bridge 1	0.6	2.946	0.0627	2.927	0.6	3.607	5.0
Bridge 2	0.815	0.447	2.5	4.375	0.815	3.762	5.413
Bridge 3	0.545	0.229	0.108	1.767	0.545	0.882	2.427
Bridge 4	0.717	0.436	0.027	3.156	0.717	1.179	4.09
Bridge 5	0.406	0.448	0.049	1.783	0.406	0.903	2.412

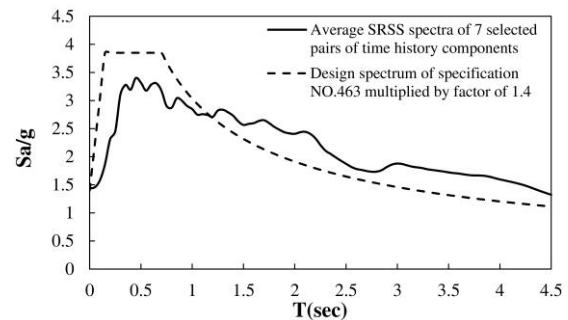


Fig. 7 Comparing the average SRSS spectrum of the chosen ground motion time-histories with the earthquake design spectrum of Specification No. 463 for soil type III

taking the square root of the sum of squares of the 5%-damped spectra of each component.

c) The spectrum of the ensemble of earthquakes shall be formed by taking the average value of the SRSS spectra of the individual earthquakes of the previous step.

d) The ensemble spectrum shall be scaled so that it is not lower than 1.4 times the 5% damped standard design spectrum for soil type III, in the period range between $0.2T_1$ and $1.5T_1$, where T_1 is the natural period of the fundamental mode of the structure.

e) The determined scale factor shall be multiplied by the scaled accelerograms in step “a” for conducting time-history analysis.

Fig. 7 indicates the average SRSS spectrum and the earthquake design spectrum for 5% damping ratio. By comparing two spectra in Fig. 7, between the periods $0.2T_1$ and $1.5T_1$, a scale factor of 1.34 is obtained. By multiplying this scale factor by the scaled selected ground acceleration time-histories, the seismic records to conduct the nonlinear time-history analyses are obtained.

6. R factor for the bridge with ERB isolator

A flowchart of the process for computing the bridge

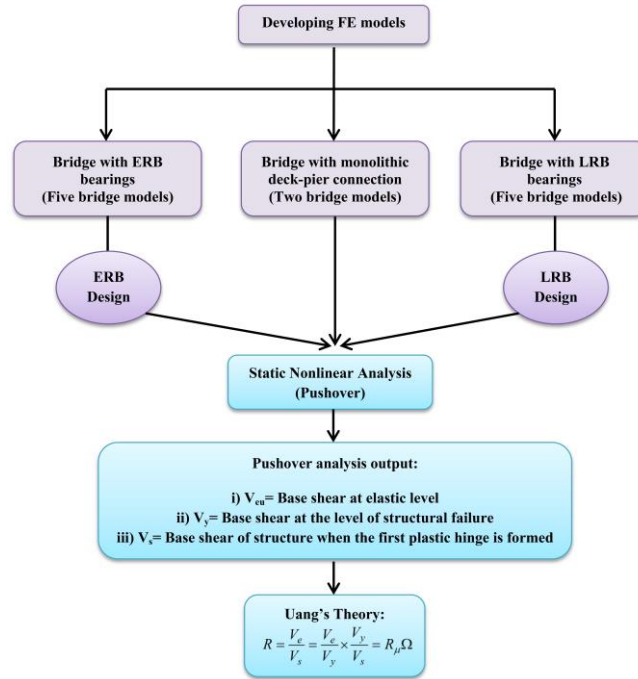


Fig. 8 Flowchart of computing *R*-factor

models’ *R*-factors is presented in Fig. 8. Based on the ERB parameters in Table 3, nonlinear static analyses are performed on the bridge models with the ERB isolator and their *R*-factors values are computed.

Values of *R*-factors, reduction factor due to ductility (R_{μ}), and the over-strength factor (Ω), in both longitudinal and transverse directions calculated according to the Uang’s approach are presented in Tables 9-10. As illustrated in these tables, the average values of *R*-factor in the cases using ERB are obtained as 3.89 and 4.91 in the longitudinal and transverse directions, respectively. The calculated *R* values do not collaborate with the specified *R*-factors in AASHTO guide specifications for seismic isolation design (i.e., $R=3/2=1.5$ for the longitudinal direction and $R=5/2=2.5$ for the transverse direction). This inconsistency is attributed to the linear behavior of ERB and absence of energy dissipation at bearing level, which cause the identical seismic forces generated in the deck to be transferred from superstructure to substructure through elastomeric bearing. As a consequence, plastic hinge formation due to the greater seismic forces in columns leads to stiffness reduction and ductility enhancement, resulting in an increase in the reduction factor due to ductility (R_{μ}). Results imply that the code-prescribed *R* values are conservative for typical bridges with ERB isolators. This result is of concern because of economic costs and it is an area that merits further investigation.

7. R factor for the bridges with LRB isolator

Based on the isolator design parameters in Table 7, *R*-factors of the bridge models with LRB isolators are computed using nonlinear static pushover analysis. Values for *R*, reduction factor due to ductility (R_{μ}), and the over-

Table 9 *R*-factor of bridges with ERB in the longitudinal direction

X-Dir	Bridge.1	Bridge.2	Bridge.3	Bridge.4	Bridge.5	Bridge.6	Bridge.7	Average
<i>T</i> (sec)	1.441	1.407	0.958	1.466	1.176	0.596	0.255	-
R_{μ}	2.485	2.504	3.697	2.037	2.59	1.33	2.474	2.44
Ω	1.325	1.77	1.556	1.879	1.59	1.8	2.474	1.62
<i>R</i>	3.292	4.43	5.75	3.83	4.12	2.4	3.43	3.89

strength factor (Ω) in both longitudinal and transverse directions are presented in Tables 11- 12. The tables reveal that the calculated average values of *R*-factors for the isolated bridges with LRB are equal to 1.652 and 2.232 in the longitudinal and transverse directions, respectively. According to the AASHTO guide specifications for seismic isolation design, the response modification factors are in the range of 1.5 to 2.5, and the reduction factor due to ductility is near unity. Comparing the results shows a good agreement between the calculated *R*-factors of this study and the specifications.

Decrease in the *R*-factor values of the isolated bridges with LRB with nonlinear behavior compared to the bridges with ERB with linear behavior is due to the philosophy of using LRB isolators. Using LRB isolator in a structure has two substantial effects including period and damping enhancement. In bridges with LRB, yielding of the lead core results in reduction of seismic force transferred from superstructure to substructure. Regarding Tables 9-12, structural period of bridges with LRB is greater than that of bridges with ERB. As a consequence, base shear at elastic level (V_e) decreases with increase in period (regarding $T>0.7sec$ “constant-velocity region in response spectrum” in Fig. 4), which leads to increase in *R*-factor value of bridges with ERB compared to that of bridges with LRB.

Table 10 R-factor of bridges with ERB in the transverse direction

Y-Dir	Bridge.1	Bridge.2	Bridge.3	Bridge.4	Bridge.5	Bridge.6	Bridge.7	Average
$T(sec)$	1.276	1.235	1.099	1.256	0.977	0.442	0.34	-
R_{μ}	2.503	3.124	3.639	3.373	3.15	1.33	1.56	2.67
Ω	2.685	1.904	1.235	2.011	1.77	2.11	1.28	1.86
R	6.722	5.95	4.5	6.78	5.57	2.82	2.0	4.91

Table 11 R factor of the isolated bridges in longitudinal direction

X-Dir	Bridge.1	Bridge.2	Bridge.3	Bridge.4	Bridge.5	Average
$T(sec)$	2	2.24	1.145	2.5	1.67	-
R_{μ}	0.93	1.04	1.07	1.35	1.48	1.174
Ω	1.28	1.34	1.54	1.44	1.43	1.406
R	1.18	1.4	1.64	1.94	2.1	1.652

Table 12 R factor of the isolated bridges in transverse direction

Y-Dir	Bridge.1	Bridge.2	Bridge.3	Bridge.4	Bridge.5	Average
$T(sec)$	1.79	2.05	1.262	2.21	1.535	-
R_{μ}	0.97	1.14	1.19	1.53	1.17	1.2
Ω	2.64	1.85	1.19	1.96	1.77	1.882
R	2.57	2.11	1.42	3	2.06	2.232

8. Base shear comparison of bridges with ERB and LRB isolators

In order to evaluate the advantages of using seismic isolation system, the maximum base shear values obtained from the time history analyses for five bridge models in two cases of using either LRB isolator or ERB isolator, as well as the percentage reductions in base shear are indicated in Figs. 9-13. A significant decrease in base shear of the isolated bridges with LRB is observed compared to the case of using ERB in both longitudinal and transverse directions. As an example, variation in base shear of bridge model 1 in two cases of using LRB and ERB isolators during the ‘‘Tabas’’ earthquake is illustrated in Fig. 14.

9. Comparing the seismic energy dissipation

In order to compare the energy dissipation mechanism of bridges with ERB and LRB isolators, nonlinear time-history analyses are carried out. Due to the large mass of superstructure, the inertial forces are transferred from superstructures to substructure through bearings during an earthquake. Hysteretic performance of LRB isolator is

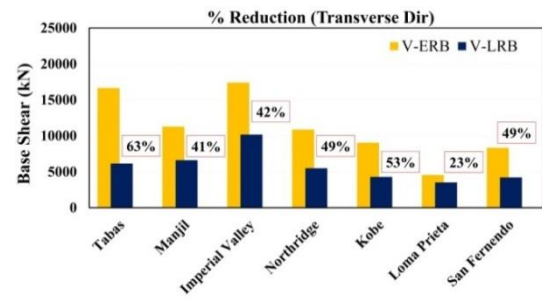
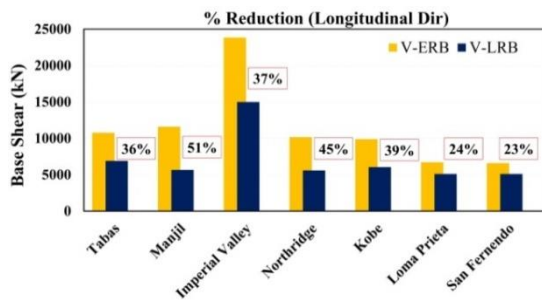


Fig. 9 Base shear comparison and percentage reduction in two cases of bridge model 1 with LRB and ERB isolators

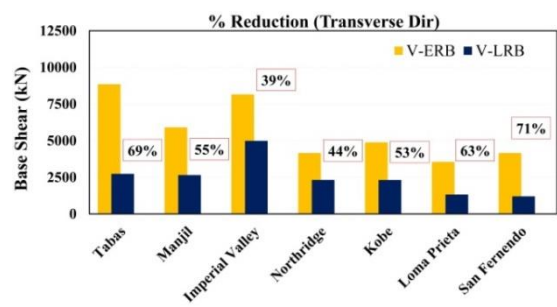
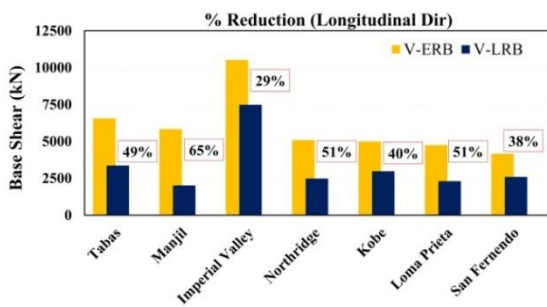


Fig. 10 Base shear comparison and percentage reduction in two cases of bridge model 2 with LRB and ERB isolators

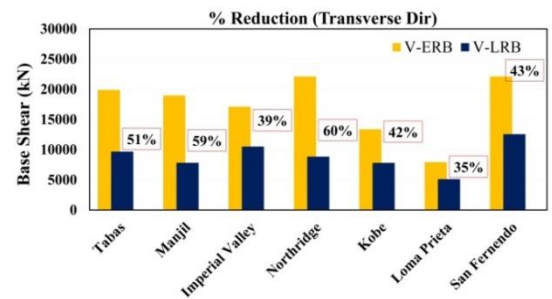
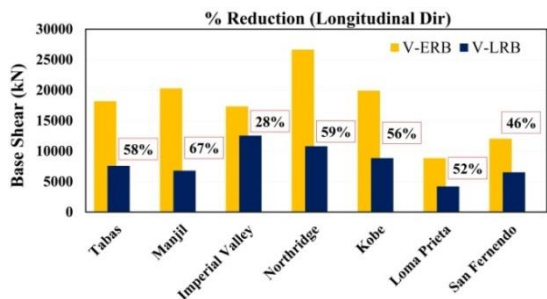


Fig. 11 Base shear comparison and percentage reduction in two cases of bridge model 3 with LRB and ERB isolators

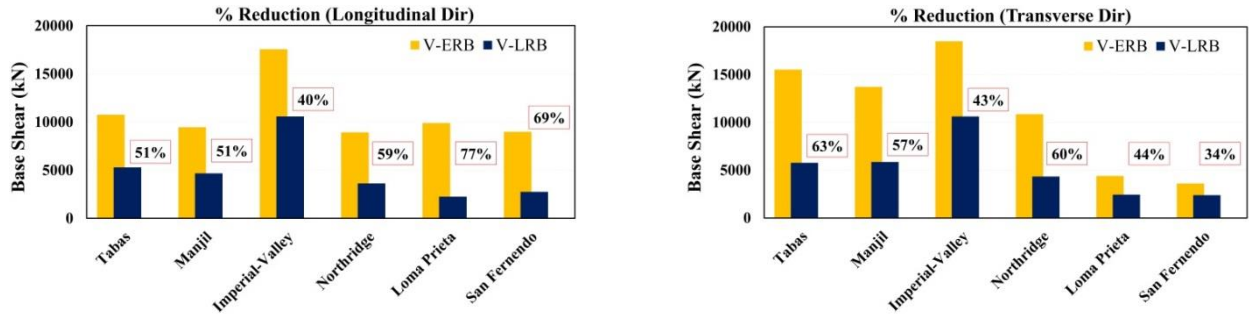


Fig. 12 Base shear comparison and percentage reduction in two cases of bridge model 4 with LRB and ERB isolators

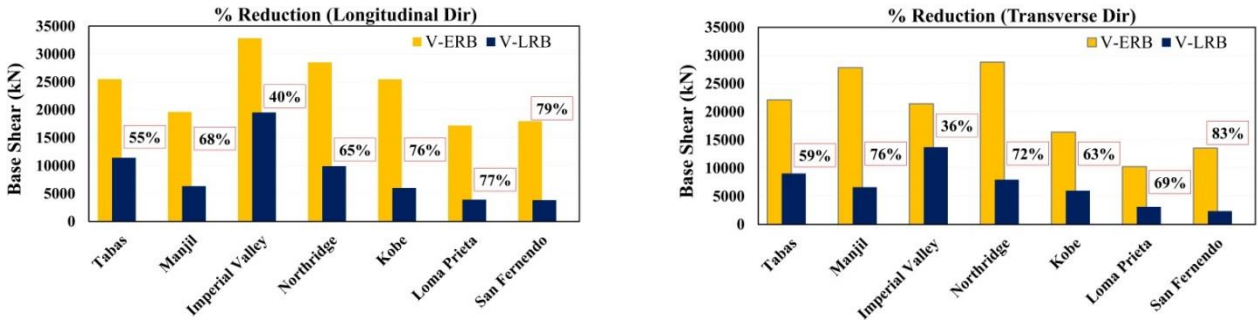


Fig. 13 Base shear comparison and percentage reduction in two cases of bridge model 5 with LRB and ERB isolators

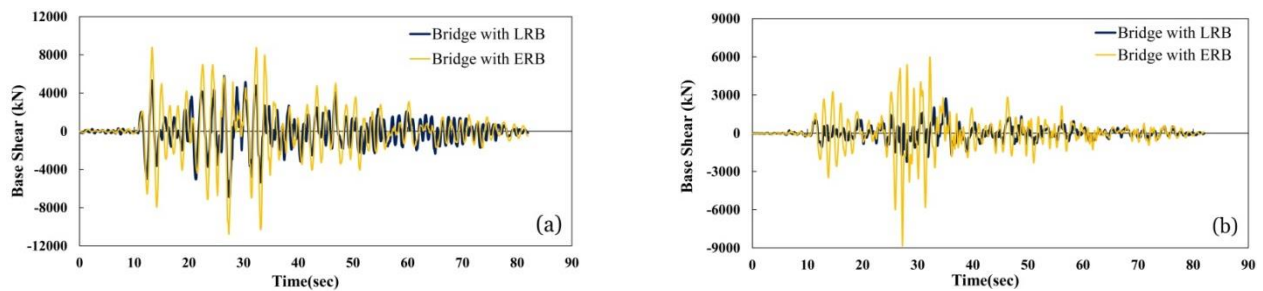


Fig. 14 Base shear of bridge model 1 under the "Tabas" earthquake in (a) longitudinal and (b) transverse directions

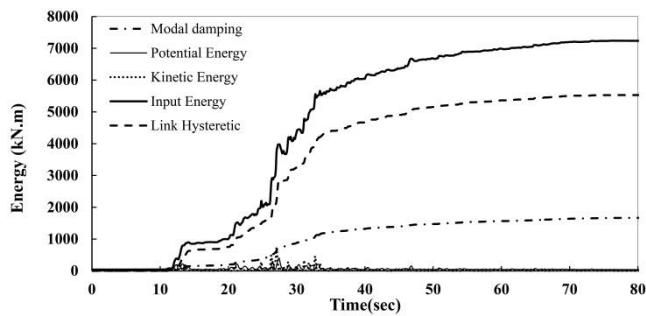


Fig. 15 Energy dissipation of bridge model 1 with LRB isolator under the "Tabas" earthquake in the longitudinal direction

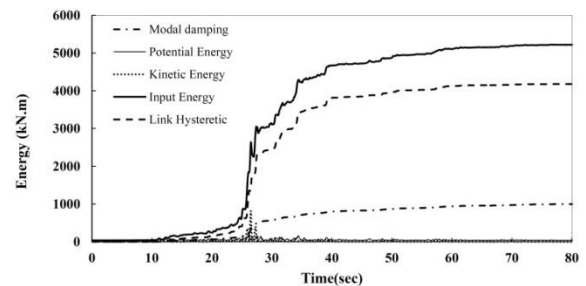


Fig. 16 Energy dissipation of bridge model 1 with LRB isolator under the "Tabas" earthquake in the transverse direction

dependent on its stiffness and damping. As shown in Figs. 15-16, the earthquake input energy in the isolated bridges with LRB is dissipated in terms of the link hysteretic, modal damping, kinetic energy, and potential energy.

However as demonstrated in Figs. 17-18, the link hysteretic term is missing in the bridges with ERB isolator because of linear behavior of ERB, and the seismic input energy is mainly dissipated as a result of modal damping due to formation of plastic hinges in columns. As observed

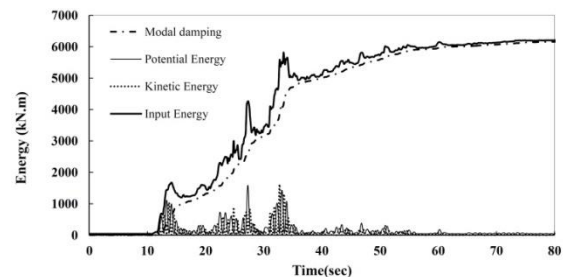


Fig. 17 Energy dissipation of bridge model 1 with ERB under the Tabas earthquake in the longitudinal direction

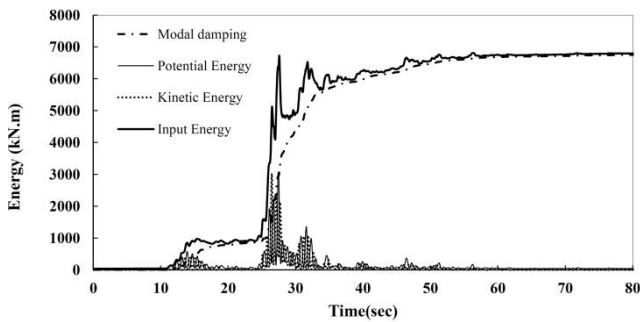


Fig. 18 Energy dissipation of bridge model 1 with ERB under the "Tabas" earthquake in the transverse direction

in bridge model 1 with LRB in Fig. 15, about 75% and 20% of seismic input energy in the longitudinal direction is dissipated through the isolation system's hysteretic energy (link hysteretic) and modal damping, respectively. Also in the transverse direction roughly 80% and 18% of the earthquake input energy are dissipated by the isolator's hysteretic energy (link hysteretic) and modal damping, respectively (see Fig. 16).

But in the bridges with ERB the major source of seismic energy dissipation is the modal damping (see Figs. 17 and 18). As an example of the link hysteretic energy dissipation, response of the LRB isolator for the bridge model 1 is depicted in Fig. 19.

Purpose of comparing energy dissipation figures is to indicate how the bridges with ERB and LRB isolators dissipate energy during an earthquake. The results of nonlinear time history analyses using the selected ground motion records for all bridge models have shown the same energy dissipation trend; in such a way that in bridges with ERB and LRB, modal damping and link hysteretic energy are the major sources of seismic input energy dissipation.

10. Conclusions

This research is intended to explore the R -factor value of isolated bridges with ERB (linear behavior), and LRB isolators (nonlinear behavior). Therefore five existing bridges with ERB and LRB isolators between superstructure and substructure are developed. Furthermore, R -factor values of two existing bridges with monolithically deck-to-pier connection are assessed.

Due to the high rigidity of bridge superstructure, substructure is responsible for ductility and energy dissipation. Hence, type of substructure (wall-type pier, single columns, multiple column-bents, etc.), superstructure-substructure connection type (monolithic, or isolated), and bearing behavior (linear, nonlinear) play the most important role in energy dissipation mechanism and ductility of the whole bridge system. Existence of an energy dissipating system such as LRB results in reduction of R -factor. This means that ductility of the substructure is decreased and it tends to behave linearly. Substructure of isolated bridges with LRB is expected to have less ductility, and the majority of energy dissipation occurs at the bearing level.

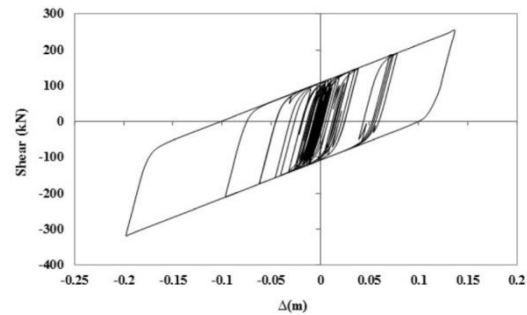


Fig. 19 Hysteresis loops of LRB isolator in bridge model 1 under the "Tabas" earthquake in the longitudinal direction

In bridges with ERB regarding to the absence of energy dissipation at the bearing level, seismic forces are transferred to the substructure without any reduction, and energy is dissipated through the formation of plastic hinges in the columns. Hence, it is necessary for the substructure of this kind of bridges to have a more ductile behavior in comparison with the bridges with LRB. Increase in the ductility leads to enhancement of R -factor values.

In two voided slab bridge models studied in the present work, R -factor in the longitudinal direction is similar to that of the non-isolated bridges. However, rigidity of piers in the transverse direction causes such bridges behave similar to those with wall-type pier in the transverse direction having lower R -factors. But still there is a need for more research in this topic to investigate how the pier sections, the space between columns in the transverse direction, and the height of columns affect the R -factor values. The results of this study can be concluded as follows:

- The average values of R -factors for the bridges with ERB are calculated as 3.89 and 4.91 in the longitudinal and transverse directions, respectively. The calculated R values mismatch the prescribed R -factors in AASHTO guide specifications for seismic isolation design (i.e., $R=3/2=1.5$ in the longitudinal direction and $R=5/2=2.5$ in the transverse direction). Results imply that the code-prescribed R values are conservative for typical bridges with ERB isolators.
- The calculated average values of R -factors for the isolated bridges with LRB are equal to 1.652 and 2.232 in longitudinal and transverse directions, respectively, that agree well with the R -factors in the AASHTO guide specifications for seismic isolation design.
- For the bridges with monolithic pier-deck connection, the average calculated R -factor in longitudinal direction is obtained as 2.92, which is close to the specified R -factor in bridge design codes; while in the transverse direction it is obtained as 2.41, i.e., about half the R -factor values in specifications.
- Base shear of the isolated bridges with LRB induced by the selected seismic motions has shown a reduction ranging from 23% to 79% in the longitudinal direction, and 23% to 83% in the transverse direction, respectively compared to the case of using ERB.
- The earthquake input energy in isolated bridges with LRB is dissipated in terms of LRB isolator's hysteretic energy (link hysteretic). However, this term is missing

in bridges with ERB isolator because of ERB's linear behavior and the seismic energy is mainly dissipated due to the modal damping through large deformation.

- Decrease in R -factor of the isolated bridges with LRB leads to a strong and stiff linear substructure. Therefore, bridge design engineers tend to consider the nonlinear behavior of the whole bridge structure in the seismic isolation system. Hence by using LRB isolator as a structural control system, response of the structure during earthquakes can be controlled. But in the case of using ERB as the seismic isolation system, the nonlinear behavior of the structure stems from the formation of plastic hinges in the piers.

References

- Al-Anany, Y.M., Moustafa, M.A. and Tait, M.J. (2017), "Modeling and evaluation of a seismically isolated bridge using unbonded fiber reinforced elastomeric isolators", *Earthq. Spectra*, **4**(1), 145-168.
- American Association of State Highway and Transportation Officials (AASHTO) (1996), Standard Specifications for Highway Bridges, 16th Edition, Washington, DC, USA.
- American Association of State Highway and Transportation Officials (AASHTO) (2014), Guide Specifications for Seismic Isolation Design, 4th Edition, Washington, D.C, USA.
- Aviram, A., Mackie, K.R. and Stojadinovic, B. (2008), "Guidelines for Nonlinear Analysis of Bridge Structures in California", *PEER 2008/03*, Pacific Earthquake Engineering Research Center.
- Caltrans (2010), Caltrans Seismic Design Criteria Version 1.6, California Dept. of Transportation, Sacramento, CA.
- Constantinou, M.C. and Quarshie, J.K. (1998), "Response modification factors for seismically isolated bridges", Rep. MCEER-98-0014, State Univ. of New York, Buffalo, NY.
- CSiBridge (2015), 17.3.0, [Computer Software], Computers and Structures, Inc., CA, USA
- European Committee for Standardization (CEN) (2005), Design of Structures for Earthquake Resistance-Part 2: Bridges, Eurocode 8, EN 1998-2, Brussels.
- Itani, A., Gaspersic, P. and Saiidi, M. (1997), "Response modification factors for seismic design of circular reinforced concrete bridge columns", *Struct. J.*, **94**(1), 23-30.
- Kappos, A.J., Paraskeva, T.S. and Moschonas, I.F. (2013), "Response modification factors for concrete bridges in Europe", *J. Bridge Eng.*, **18**(12), 1328-1335.
- Kelly, J.M. (1997), *Earthquake-Resistant Design with Rubber*, 2nd Edition, Springer, London, U.K.
- Losanno, D., Spizzuoco, M. and Serino, G. (2014), "Optimal design of the seismic protection system for isolated bridges", *Earthq. Struct.*, **7**(6), 969-999.
- Memari, A., Harris, H., Hamid, A. and Scanlon, A. (2005), "Ductility evaluation for typical existing R/C bridge columns in the eastern USA", *Eng. Struct.*, **27**, 203-212.
- Naeim, F. and Kelly, J.M. (1999), *Design of Seismic Isolated Structures; From Theory to Practice*, John Wiley and Sons, Chichester, England.
- Nagarajaiah, S., Reinhorn, A.M. and Constantinou, M.C. (1991), "Nonlinear dynamic analysis of 3-D base-isolated structures", *J. Struct. Eng.*, **117**(7), 2035-2054.
- Olmos, B.A. (2008), "Nonlinear seismic response of Mexican bridges with base isolation accounting for soil structure interaction effects", Ph.D. Dissertation, Texas A&M University, Texas, U.S.
- Olmos, B.A., Jara, J.M. and Roesset, J.M. (2011), "Effects of isolation on the seismic response of bridges designed for two different soil types", *Bull. Earthq. Eng.*, **9**(2), 641-656.
- Park, Y.J., Ang, A.H.S. and Wen, Y.K. (1986), "Random vibration of hysteretic systems under bi-directional ground motions", *Earthq. Eng. Struct. Dyn.*, **14**(4), 543-557.
- Saiidi, M., Maragakis, E. and Griffin, G. (1999), "Effect of base isolation on the seismic response of multi-column bridges", *Struct. Eng. Mech.*, **8**(4), 411-419.
- Skinner, R.I., Robinson, W.H. and McVerry, G.H. (1993), *An Introduction to Seismic Isolation*, John Wiley & Sons Ltd, Chichester, England.
- Soares, R.W., Lima, S.S. and Santos, H.S.C. (2017), "Reinforced concrete bridge pier ductility analysis for different levels of detailing", *IBRACON Struct. Mater. J.*, **10**(5), 1042-1050.
- Specification No. 139 (2000), Standard Loads for Bridges, Ministry of Roads and Transportation, Office of the Deputy for Technical Affairs, Tehran, Iran.
- Specification No. 463 (2008), Road and Railway Bridges Seismic Resistant Design Code, Ministry of Roads and Transportation, Deputy of Training; Research and Information Technology, Tehran, Iran.
- Toopchi-Nezhad, H. (2014), "Horizontal stiffness solutions for unbonded fiber reinforced elastomeric bearings", *Struct. Eng. Mech.*, **49**(3), 395-410.
- Uang, C.M. (1991), "Establishing R (or R_w) and C_d factors for building seismic provisions", *J. Struct. Eng.*, **117**(1), 19-28.
- Wen, Y.K. (1976), "Method for random vibration of hysteretic systems", *J. Eng. Mech.*, **102**(2), 249-263.

CC